The United Nations University

GEOTHERMAL TRAINING PROGRAMME
Orkustofnun, Grensásvegur 9,
IS-108 Reykjavík, Iceland

Reports 2006
Number 19

AMORPHOUS IRON SILICATE SCALES IN SURFACE PIPELINES: CHARACTERIZATION AND GEOCHEMICAL CONSTRAINTS ON FORMATION CONDITIONS IN THE MIRAVALLES GEOTHERMAL FIELD, COSTA RICA

Alejandro Rodríguez
Instituto Costarricense de Electricidad (ICE)
Centro de Servicio de Recursos Geotérmicos
Guayabo de Bagaces, Guanacaste
COSTA RICA
arodriguezba@ice.go.cr

ABSTRACT

Scales, formed in surface pipelines as a result of mixing of neutral and acidic fluids at the Miravalles geothermal field, have been characterized by chemical analysis, X-ray diffraction (XRD), scanning electron microscopy (SEM) and energy dispersive X-ray spectrometry (EDS). They consist of a chemically homogeneous amorphous iron silicate with a stoichiometry similar to the mineral minnesotaite ($(Fe^{++},Mg)_3Si_4O_{10}(OH)_2$). With the aid of computer programs for geochemical aqueous speciation (WATCH and EQ3NR) and for reaction path modelling of aqueous geochemical systems (EQ6), the geochemical constraints of the formation of the scales were modelled. The mixing experiments simulated with EQ6 between neutral and acidic fluids, determined a range of log *K* for the dissolution reaction of the scale phase, $6H^+ + Fe_3Si_4O_{10}(OH)_2 \leftrightarrow 3Fe^{2+} + 4SiO_2 + 4H_2O$, lies between 11 and 13 at 195°C. Above this range, the probabilities of over saturation of this compound are very high. On the basis of a series of mixing scenarios, acidification of neutral fluids to a pH value of 6.0 is suggested in order to prevent the formation of these scales.

1. INTRODUCTION

1.1 General aspects of the Miravalles geothermal field

Costa Rica is located in the southern part of Central America, in the subduction zone of the Cocos Plate beneath the Caribbean Plate. That interaction has generated an internal magmatic arc in which the Guanacaste Volcanic Cordillera comprises the northwest segment (Figure 1). The Miravalles geothermal field is located in the northwest part of Costa Rica on the southwest flank of the Miravalles volcano, within a 14 km diameter semi-circular structure known as the Guayabo caldera.

Ten stratigraphic units related to the formation and the filling of the caldera, including pyroclastic materials, lavas, debris avalanches and lacustrine deposits, dating from Miocene to Holocene are described by Vega et al. (2005). The permeability of the field is mainly secondary in nature, controlled by fault systems striking NW-SE, N-S, NE-SW and E-W.

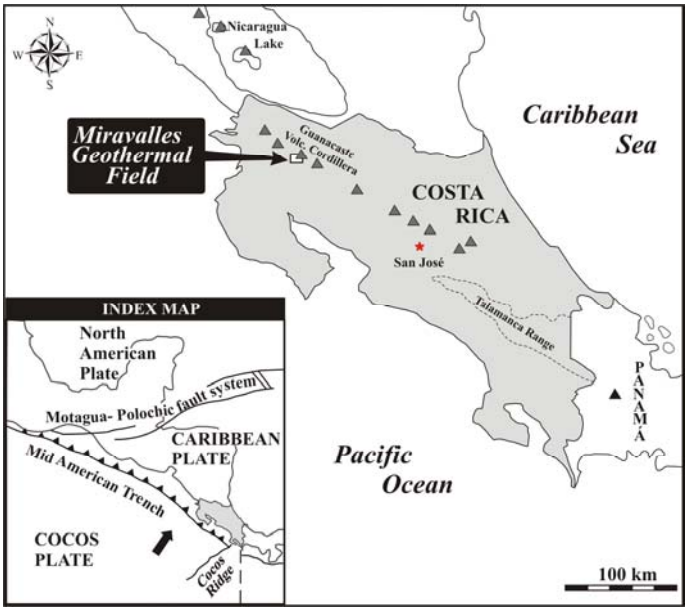

FIGURE 1: Location map (modified from Vega et al., (2005)

The geothermal reservoir is a high-temperature and liquid-dominated type. Its heat source is related to the nearby Miravalles volcano. The reservoir is encountered at about 700 m depth and its temperatures decline towards the south and west. The estimated thickness of the reservoir is about 800–1,000 m, and it has a temperature range from 230 to 255°C (Sánchez et al., 2005).

Deep drilling at Miravalles started in 1979, when a high-temperature reservoir was discovered. Subsequent drilling stages provided steam to three single flash plants commissioned in 1994, 1998 and 2000, and one binary plant in 2004, totalling an installed capacity of 163 MWe. Three backpressure units of 5 MWe each have produced for different periods, and one of them is still producing and belongs to ICE (Instituto Costarricense de Electricidad). Table 1 shows the installed electrical capacity at Miravalles. At the end of 2004, that installed capacity was 8.4% of the total installed capacity of Costa Rica, and the energy produced at Miravalles during the same year represented about 15.1% of the total electrical energy produced in the country (ICE, 2004; Mainieri, 2005).

TABLE 1: Miravalles geothermal field, installed capacity

Unit	Generation (MWe)	Type	Start	Owner
Miravalles 1	55	SF	March, 1994	ICE
BPU	5	BP	January, 1995	ICE
Miravalles 2	55	SF	August, 1998	ICE
Miravalles 3	29.5	SF	March, 2000	BOT
Miravalles 5	18	ORC	December, 2003	ICE

SF = Single flash; BP = Backpressure;
BOT = Build-operate-transfer; ORC = Organic Rankine Cycle.

At Miravalles, 52 wells have been drilled, 30 of them are or could be used for producing steam and 13 for brine reinjection. Among the production wells, 5 produce acidic fluids; 4 of them are now producing by means of deep neutralization. The total production of the wells in Miravalles is about 300 kg/s of steam, and about 1350 kg/s of brine (of which 800 kg/s are used for a binary plant) are injected back to the reservoir.

1.2 Chemical characteristics of the different types of fluids

At Miravalles there are four different geothermal aquifers. A shallow steam-dominated aquifer is located in the northeast part of the field (Vallejos, 1996). The other aquifers are described below. Their locations are shown in Figure 2 and their chemical characteristics are summarised in Table 2.

Neutral sodium-chloride aquifer (Na-Cl). The neutral sodium-chloride aquifer is located at the northern and central sectors of the field. It is the most important in terms of production. The fluids from this aquifer have a sodium-chloride composition. After flashing at 98°C and cooling to an

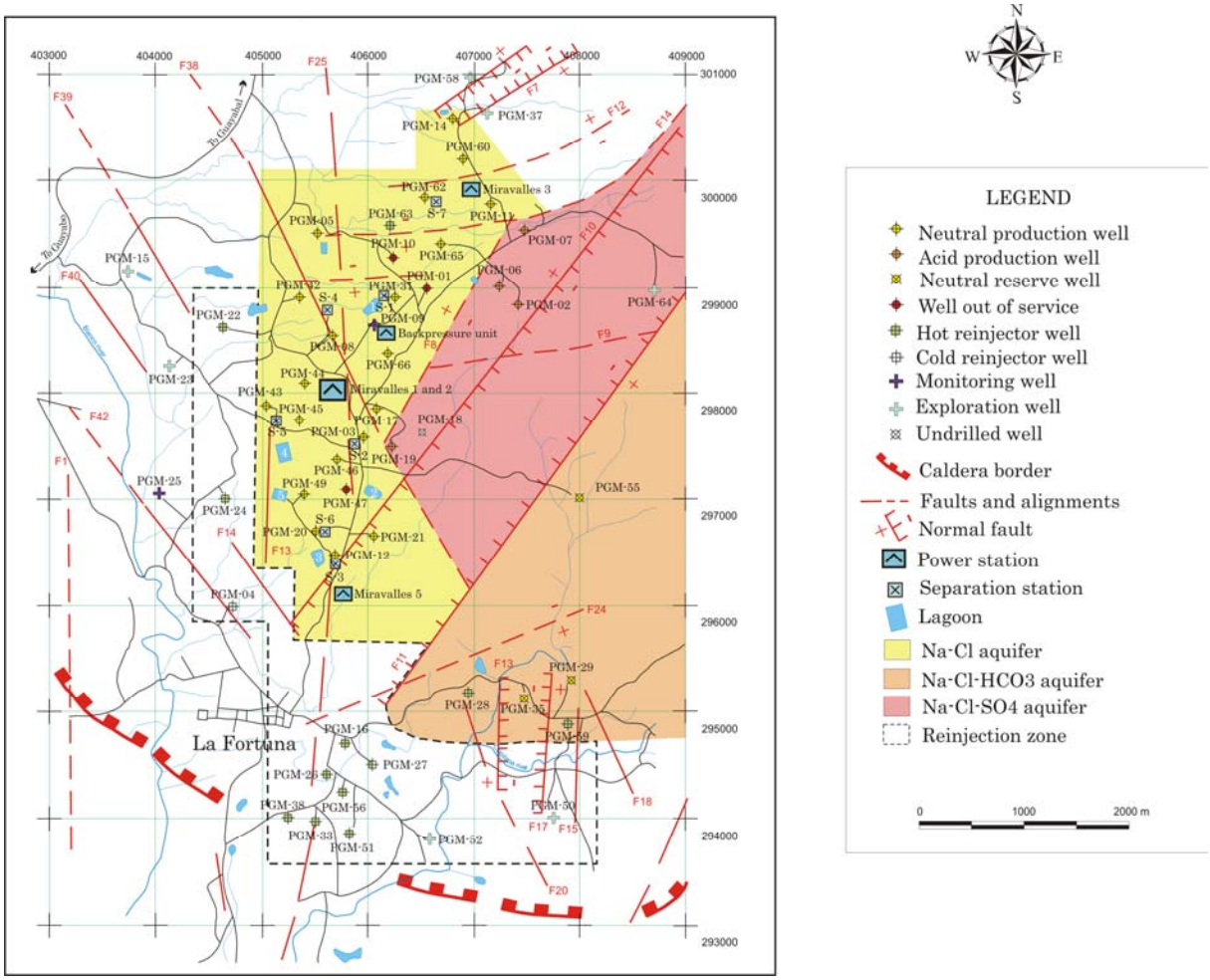

FIGURE 2: Miravalles geothermal field

ambient temperature, pH values are from 7.6 to 8.0, chloride content from 4,100 to 5,000 ppm, silica from 580 to 620 ppm, calcium from 70 to 130 ppm, bicarbonate from 15 to 70 ppm, and TDS (total dissolve solids) between 8,000 and 10,000 ppm. Calcium carbonate ($CaCO_3$) scaling has been observed in production wells in this sector of the field. These scales could result in complete obstruction of the wells ranging from weeks to several months if an inhibition system was not employed.

TABLE 2: Chemical characteristics of the deep aquifers at Miravalles

Aquifer	pH	Cl (ppm)	HCO_3 (ppm)	SO_4 (ppm)	Ca (ppm)	SiO_2 (ppm)	TDS (ppm)
Na-Cl	7.6 – 8.0	4,100 – 5,000	15 - 70	50 - 60	70 - 130	580 - 620	8,000 – 10,000
Na-Cl-HCO3	7.4 – 8.2	4,000 – 4,300	160 - 215	66 - 80	60 - 70	550 - 560	8,000 – 8,400
Na-Cl-SO4	2.4 – 3.2	3,900 – 4,300	0 - 2	170 - 300	35 - 50	550 - 650	7,240 – 7,395

Neutral sodium-chloride-bicarbonate aquifer (Na-Cl-HCO_3). The neutral sodium-chloride-bicarbonate aquifer is located in the southeast sector of the field. The fluids have a sodium-chloride-bicarbonate composition. After flashing at 98°C and cooling to ambient temperature, pH values are between 7.4 and 8.2, chloride content from 4,000 to 4,300 ppm, bicarbonate from 160 to 215 ppm, silica from 550 to 560 ppm, calcium from 60 to 70 ppm, and TDS between 8,000 and 8,400 ppm. The $CaCO_3$ scaling tendency of these wells is severe. Production from these wells without inhibition systems would clog the casing in a matter of a few days.

Acid sodium-chloride-sulphate aquifer (Na-Cl-SO_4). The acid sodium-chloride-sulphate aquifer is located in the northeast sector of Miravalles. The fluids from this aquifer have a sodium-chloride-sulphate composition. After flashing at 98°C and cooling to ambient temperature, pH values are between 2.4 and 3.2, chloride content from 3,900 to 4,300 ppm, sulphate from 170 to 300 ppm, silica from 550 to 650 ppm, calcium from 35 to 50 ppm, bicarbonate from 0 to 2 ppm, and TDS between 7,240 and 7,395 ppm. Without an appropriate neutralization system, the corrosive character of these fluids would rapidly cause catastrophic and irreparable damage to the well casings and surface equipment.

In summary, it can be said that the commercial exploitation of fluids at Miravalles would be impossible without the application of deep chemical treatments in the wells. However, although calcite scaling and corrosion problems can be prevented in individual wells, scaling is still a problem where neutralized acidic fluids come into contact with fluids from the neutral wells. This investigation is intended to study the composition of these scales, explain their formation mechanisms, and to propose a solution to the problem.

1.3 Objectives of this study and applications

The formation of scales on equipment surfaces exposed to geothermal fluids can have serious economic consequences arising from energy losses, increased cost of cleaning and maintenance, loss of production, or even abandonment of a production well. In recent years, considerable effort has been made worldwide to characterise geothermal scale deposits.

The objectives of this work are:

- To chemically characterise scales formed as a result of the mixing of neutral and acidic fluids, mainly between wells PGM-66 and PGM-17, on one hand, and PGM-19 on the other.

- To define the geochemical constraints and the formation mechanisms of the scales and to model those with the aid of geochemical speciation and reaction path programs.

- To suggest measures for mitigating the problem.

The results of this work are an improved understanding of acidic geothermal fluids in order to mitigate the problems that arise as a result of their use. This is of considerable importance since at Miravalles, 4 acidic wells (PGM-02, PGM-06, PGM-07 and PGM-19) produce the equivalent of 30 MWe, which is a significant portion of the total production at Miravalles. Also, in the near future, the exploitation of the acid aquifer could be extended in order to satisfy steam requirements, mainly in the northern zone for the Miravalles 3 power station.

2. UTILIZATION OF ACID FLUIDS AND THEIR SECONDARY EFFECTS AT MIRAVALLES

The first experiments on neutralizing acidic fluids from Miravalles wells were carried out in 1996. The neutralization process consisted of injection of a solution of sodium hydroxide (NaOH) to a depth below the casing shoe with the aid of a pump and capillary tubing. This neutralized the acids, thus raising the pH. Since February 2000 and October 2001, wells PGM-19 and PGM-07, respectively, have been neutralized successfully. Together, these wells produce a steam equivalent to approximately 17 MWe for the power plants. Logistical and scientific aspects of the commercial integration of acidic wells have been discussed by Sánchez (1997), Castro and Sánchez (1998), Sánchez et al. (2000), Moya and Sánchez (2002) and Sánchez et al. (2005). Also, during June 2006,

two more acidic wells, PGM-02 and PGM-06, were integrated into the system. Those wells produce 3.5 and 10 MWe, respectively. Thus, the power that can be obtained at Miravalles from acidic wells accounts for around 30 MWe.

The first attempts to neutralize acidic fluids resulted in scaling problems. Soon after the implementation of neutralization systems in wells PGM-19 and PGM-07, it was observed that amorphous siliceous scales were formed in a matter of months, as a result of the neutralization process. Also, similar scales formed inside the separator, water tanks and pipelines located at the site of each well. The scaling problems were so severe that mechanical cleansing had to be performed every 6 months at PGM-07. Mechanical cleansings were very expensive, risky and time consuming operations that resulted in long periods during which the well could not produce. Furthermore, after each cleaning operation, PGM-07 could not be returned to stable production conditions, partly due to cold water injection as a part of the cleaning process.

Corrosion and scaling studies performed at PGM-07 from October 2003 to March 2004, in cooperation with NEDO (New Energy and Industrial Technology Development Organization) of Japan, concluded that in order to minimize corrosion and scaling, a pH value of 5.0 inside the wells must be maintained (Rodríguez and Sánchez, 2004; NEDO, 2004). This is lower than the pH value of 6.0 that was used before. Measurements of pH, in samples collected at different separation pressures, demonstrated that a pH of 5.0 would correspond to a pH between 5.8 and 6.0 if the sample was boiled at 98°C and cooled to ambient temperature for the case of PGM-07 fluids, and to a pH between 5.5 and 5.7 for the case of PGM-19 fluids. With these small adjustments in neutralization conditions, both corrosion and scaling were minimized at depth and inside surface equipment located at the site of acidic wells.

Before the optimization of neutralization processes, the two-phase fluids from wells PGM-07 and PGM-19 were conducted to a separator located at each site. From there, the steam was sent to the power station and the brine to the cold reinjection system. Later, when the scaling and corrosion problems seemed solved, both wells were integrated directly to the separation units 7 and 2, respectively, at the end of July 2004. During a maintenance inspection performed on October 2004, it was observed that at separation unit 7 the surface equipment like separators, water tanks and pipelines were completely clean. On the other hand, at separation unit 2 ("Satélite 2"), the presence of thick, black and vitreous scales were observed inside the equipment. Furthermore, it was observed that the first occurrence of the scales was at point U-20, where fluids from wells PGM-66, PGM-17 (both neutral), and PGM-19 were mixed (Figures 3 and 4).

Although there were no scaling problems at separation unit 7, it was soon realized that a geochemical incompatibility between the neutral and acidic fluids existed. The immediate solution to this problem was to avoid the mixing between those fluids, resume separation of PGM-19 fluids at the site and send the brine through the cold reinjection system. The consequences of that change were that when the brine separated at PGM-19 was discharged at atmospheric pressure, it resulted in an over saturation of amorphous silica, creating thick deposits at the canal and surface pipelines.

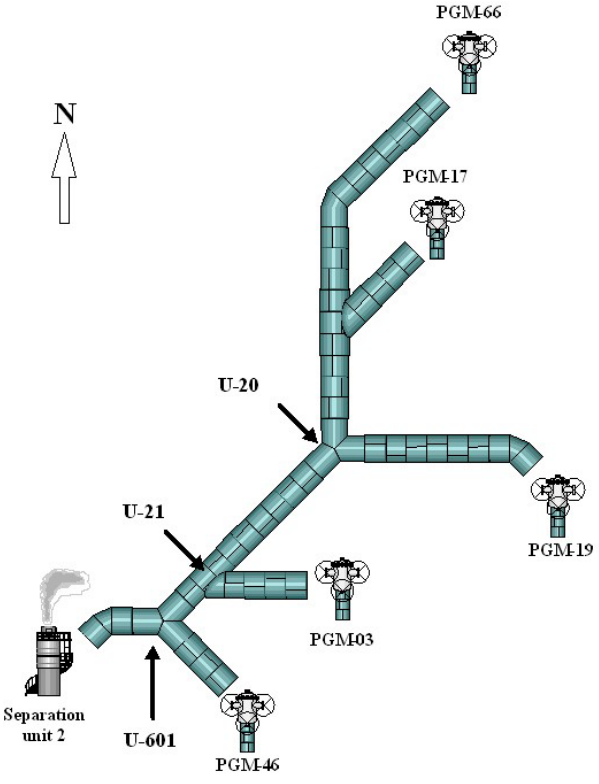

FIGURE 3: Location where scaling occurred

FIGURE 4: Site U-20, where the mixing between neutral and acid fluids occurred

3. AMORPHOUS IRON SILICATE SCALES, FORMATION AND OCCURRENCE

The great complexity of the scale formation process results from the large number of species found in a geothermal fluid and from the multiple possible physical mechanisms involved. Furthermore, the diversity of fluid composition from site to site and the variation of processes along the flow path, make the generalization of both the mechanisms responsible for the scale formation and preventive measures difficult. The composition of scales in geothermal plants is commonly very complex and depends on many parameters, such as the temperature and pressure of the fluid, the history of water-rock interactions and the operating conditions (Andritsos and Karabelas, 1991).

Mineral scaling can be a serious problem during geothermal energy exploitation and commonly causes problems, for example: restricting fluid flow, preventing valves from closing, clogging surface pipelines and reinjection wells (Hardardóttir et al., 2005).

Many different types of precipitates from geothermal fluids have been documented and characterized. Iron-rich silicate scales are deposited from hyper saline brines produced at the Salton Sea geothermal field, California. These scales appear as brown-black, vitreous solids resembling obsidian (Gallup, 1989) and have been observed depositing in brine-handling equipment and wells at rates ranging from ~0.5 cm/yr in production wells (>200°C) to over 50 cm/yr in injection pipes and wells (150 – 175°C) (Gallup, 1993). The occurrence of similar scales has also been documented at Cerro Prieto, Mexico (Mercado *et al*., 1989), Milos, Greece (Karabelas et al., 1989), Tiwi, Philippines (Gallup, 1993) and Reykjanes, Iceland (Kristmannsdóttir, 1984; Hardardóttir, 2004; Hardardóttir, 2005 and Hardardóttir et al., 2005).

In previous studies, iron-rich scales deposited from Salton Sea geothermal brine at high temperature were shown to consist of what is believed to be a compound exhibiting an empirical formula near $Fe(OH)_3 \cdot SiO_2 \cdot xH_2O$ or $Fe_2O_3 \cdot 2SiO_2 \cdot xH_2O$ (Gallup, 1989). Spectroscopy (Mössbauer and IR) and X-ray diffraction studies undertaken at Salton Sea by Gallup and Reiff (1991) to improve the understanding of the nature of these deposits, detected mainly ferric (Fe^{3+}) but also ferrous (Fe^{2+}) iron, believed to be present as hydrous silicates resembling the mineral hisingerite and exhibiting a variable composition. According to those authors, other iron minerals were also detected and the bulk of the mineral phases present were microcrystalline, poorly-crystalline or glassy. Iron deposited in scales

appears to derive primarily from brine, but is also found to be present as poorly-crystalline steel corrosion products (Gallup and Reiff, 1991). These authors concluded that ferric iron in the scale was deposited as a result of oxidation of ferrous iron in the brine by water:

$$Fe^{2+} + 3H_2O \Leftrightarrow Fe(OH)_3 + 2H^+ + \tfrac{1}{2}H_2 \quad (1)$$

The ferric iron generated in Reaction 1 can then react with dissolved silica to form ferric silicate scale:

$$Fe(OH)_3 + Si(OH)_4 \Leftrightarrow Fe(OH)_3 \cdot SiO_2 + 2H_2O \quad (2)$$

The overall scale forming reaction appears to be a combination of Reactions 1 and 2:

$$Fe^{2+} + H_2O + Si(OH)_4 \Leftrightarrow Fe(OH)_3 \cdot SiO_2 + 2H^+ + \tfrac{1}{2}H_2 \quad (3)$$

Also Manceau et al. (1995), using X-ray diffraction and spectroscopic techniques, confirmed that high-temperature (250°C) scale precipitated from non-oxidized geothermal brines at Salton Sea contains polymerized ferric iron and silica and identified the mineralogical nature of this precipitate as hisingerite. Hisingerite is a poorly-crystallized, non-stoichiometric nontronite. Furthermore, they identified a low-temperature (100°C) scale precipitated form the same brines as a mixture of A-opal and micro- or nano-crystalline hydrous ferrous silicate structurally related to minnesotaite and/or greenalite. However, these components are difficult to identify by XRD alone.

High scaling rates of ferric silicate at Salton Sea severely plagued the operation of steam-gathering facilities. More traditional methods for controlling this deposition have been unsuccessful, such as the injection of a wide variety of commercially available scale inhibitors, some of which have actually aggravated the scaling problem (Gallup, 1993). The process that has been used to prevent the scale deposition is brine acidification. In this process, a small amount of hydrochloric acid (HCl) is injected into the brine near a wellhead separator. The lowering of pH by 0.5 to 0.3 units has successfully inhibited ferric silicate formation (Hoyer et al., 1991). According to these authors, acidification of the brine is believed to: 1) increase the solubility of ferric ions and thereby decrease the driving force for precipitation either as ferric oxyhydroxide and/or 2) retard the kinetics of iron silicate polymerization reactions.

The fact that the scales became enriched in a hydrous ferrous (Fe^{2+}) silicate component as the brine temperature decreased, suggested that ferrous silicate is somewhat more soluble than the corresponding ferric (Fe^{3+}) silicate phase (Gallup and Reiff, 1991). Based on that solubility behaviour, Gallup (1993) saw the possibility of using chemical reducing agents capable of reducing trivalent iron to divalent iron as scale inhibitors. The results of a series of pilot unit tests conducted at Salton Sea, provided conclusive evidence that the addition of sodium formate (NaHCOO) effectively converted up to 99% of the ferric iron in the untreated brine to the more benign ferrous state (Gallup, 1993). Moreover, the reduction of ferric ions in geothermal brine by reducing agents is expected to have a mitigating effect on the corrosion of mild steel equipment since ferric ions are well-know corrosive agents toward many metallic construction materials (Gallup, 1993).

A major benefit of including the reducing agent in the brine pH modification process was corrosion mitigation. The addition of sodium formate with hydrochloric acid significantly reduced corrosion compared to acid injection alone. For those tests, sufficient acid was added to reduce the pH by 0.5 units and twice the stoichiometric amount of sodium formate necessary to reduce the ferric ions in the brine to a ferrous state were injected separately into the brine (Gallup, 1993).

The formation of iron silicate scales in conjunction with other scale phases also seems to occur when fluids with different chemistry are mixed. Since those fluids are in many cases geochemically incompatible, their mixtures can be supersaturated with respect to some scale phases that tend to

precipitate. For example, iron silicates in conjunction with iron oxides have been found on bacterial surfaces collected near hydrothermal vents in the northeast Pacific Ocean, where bacterial surfaces provide nucleation sites for poorly ordered oxides and silicates (Fortin et al., 1998). In that case, as high-temperature, reducing, and acidic solutions mix with sea water, various minerals precipitate around the vents. According to Todaka et al. (2003), at Onikobe geothermal field, in Japan, two types of fluids are encountered in the reservoir, one is neutral and the other acidic (pH = 3). These authors modelled mixing scenarios between those fluids and concluded that manganese-rich smectite precipitated due to mixing of the two fluids, forming an impermeable barrier that would explain why those fluids are separated in the geothermal reservoir.

4. SCALE CHARACTERIZATION

4.1 Macroscopic description of the scale

The samples collected for inspection are from sites U-20, U-21 and U-601 in the pipeline to separation unit 2 (Figure 3). U-20 corresponds to the point where neutral fluids from wells PGM-66 and PGM-17 encounter the acidic fluids from PGM-19 (Figure 4). At U-21 the fluids from PGM-03 are added to the system. Finally, at U-601, PGM-46 fluids are mixed with the ones that come from all the wells mentioned. The scales appear as a black, relatively hard solid with vitreous luster intercalated with softer light brown layers. Frequently, a transitional change exists between these layers. The thickness of a single layer is from 1 to 5 mm, and the intercalations as a whole can reach thicknesses up to 1 cm. They develop both parallel laminations and asymmetrical ripples (Figure 5). The different layers are generally difficult to separate mechanically from each other. Generally, it was observed that at U-20, the black material was more common than at U-33.

4.2 Chemical analysis

The scale samples collected were taken during the cleaning operations of the pipelines performed in October 2004. Chemical analyses performed at the ICE laboratories at Miravalles of both black and light brown layers of the scales are shown in Table 3. Those analyses were carried out on a wet basis. It can be seen that silicon and iron are the main components of the scales.

TABLE 3: Chemical analysis of the scales (based on a dry weight basis)

Site	% SiO_2 (±0.6)	% Fe_2O_3	% CaO (±0.02)	% MgO (±0.1)	% Na_2O (±0.04)	% K_2O (±0.01)
U-601 (l-b)	52.1	13.7 ± 0.3	0.81	3.9	2.66	0.28
U-601 (b)	49.6	24.6 ± 0.5	0.85	4.1	2.10	0.35
U-21 (l-b)	49.0	16.6 ± 0.3	0.85	4.7	2.68	0.26
U-21 (b)	46.1	25.3 ± 0.5	0.45 ± 0.01	2.8	1.94	0.25
U-20 (l-b)	47.3	27.7 ± 0.5	0.70	2.4	2.13	0.28

b: black layer, l-b: light brown layer

4.3 X-ray diffraction (XRD) analysis

Scale samples from both sites U-20 and U-601 were analysed with the X-ray diffraction (XRD) technique at ÍSOR (Iceland GeoSurvey) laboratories. Dark and light brown coloured layers were separated with the aid of a scalp. The solids were milled, combined with acetone to a fine powder in an agate mortar. Then the mixture was dried at ambient temperature. The powder was put into an acrylic plate and the sample was scanned in a Bruker AXS D8 Focus model diffractometer equipped with a Bragg-Brentano goniometer, and a Cu anode lamp with a NaI crystal type scintillation counter.

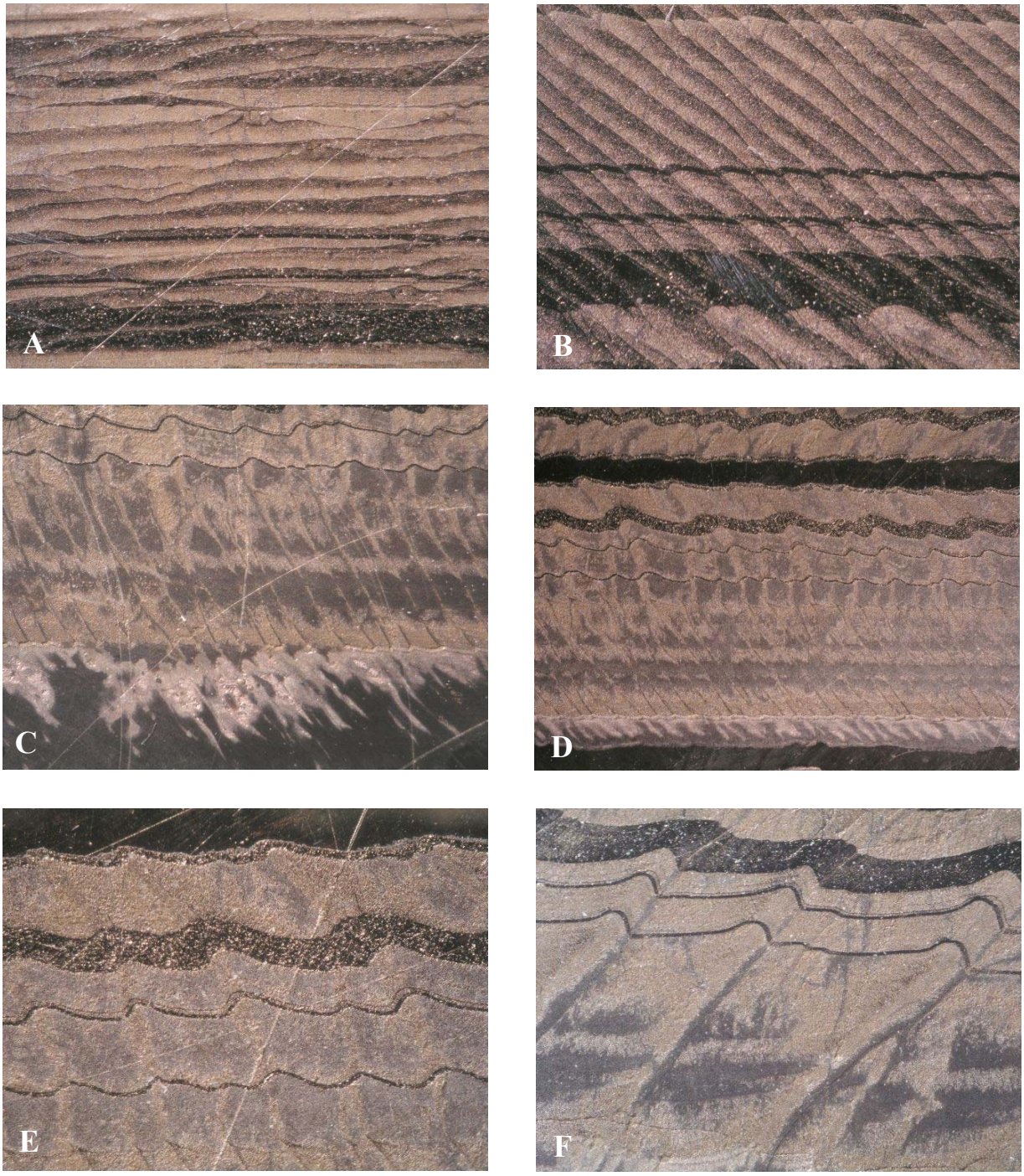

FIGURE 5: Photographs showing the structures of the scales (12.5 to 25 ×)

All samples were run in a step scan mode at 0.04°/1.0 s from 4 to 64° 2θ. The diffractograms of the scales exhibit poorly defined patterns that suggest the presence of a poorly crystallized material (Figure 6). There are a few broad humps in the patterns and this material is clearly different from amorphous silica. A typical pattern of amorphous silica is presented for comparison, but the presence of this phase in the scales analyzed is unlikely. In general terms, the black layers of the scales show a more even pattern compared to the light brown layers. Weak reflections that occur at ~7°, ~20°, ~35° and at ~60° 2θ in XRD patterns of the light brown layers, are much weaker in the XRD patterns of the black ones.

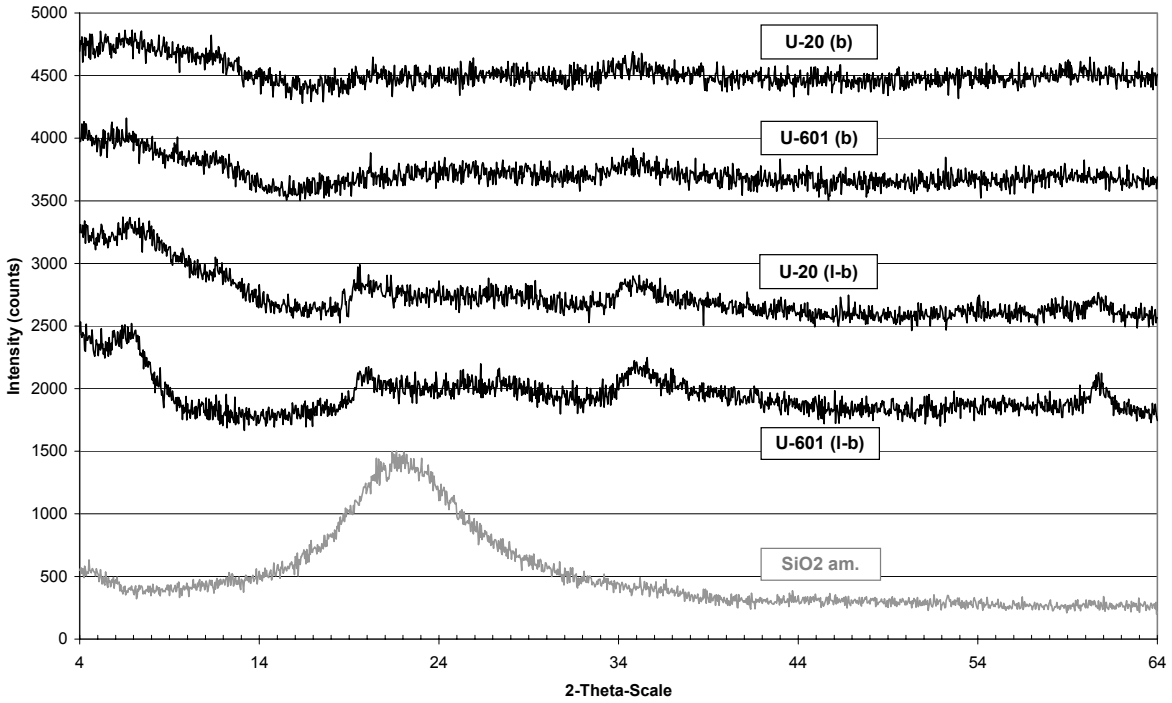

FIGURE 6: XRD patterns of scales collected at sites U-20 and U-601
(l-b: light brown, b: black; patterns offset by 1000 units)

4.4 SEM analysis of scale morphology and composition

Scanning Electron Microscopy (SEM) analyses were carried out on scale samples collected at sites U-20 and U-601. In order to study their morphology and chemical composition, small pieces of the scales were carefully embedded in epoxy resin, polished and then coated with gold before they were placed in the SEM. The analyses were performed at the Technology Institute of Iceland (IceTec). The apparatus used was a Leo Supra 25 scanning electron microscope, equipped with a Gemini field emission column and an energy dispersive X-ray spectrometer (EDS) for performing geochemical analyses. The SEM was operated at 15.00 kV accelerating voltage, 8.5 mm working distance and with a 60 μm aperture size. Prior and subsequent to analysis, cobalt (Co) standard was run in order to adjust the dead time during analysis to approximately 25% and to correct for instrument drift.

The SEM micrographs were taken with the backscatter electron detector which detects contrasts between areas of different chemical compositions in a sample. The uniform gray colour suggests that the chemical composition of the scales is homogeneous (Figure 7). Micrograph A shows that parallel laminations of scales result from a change in texture between porous and compact layers of the same material. The morphology of the asymmetrical ripples can be observed in micrograph B. Areas with a linear array, consisting of more dense material, cross those ripples by their crest. Micrograph C corresponds to a closer view of the porous layers. They seem to be formed by aggregates of particles that develop a network of chains with branches. Micrograph D shows that, in some parts, those particles become more and more compact until their identity is lost. The network structure can be appreciated in micrograph E. The size of the particles in the scales is around 1 μm. In micrograph F, it can be seen that each particle tends to bond with another by means of fibrous structures.

The formation mechanism of the scales appears consist of two stages. First, silicate particle growth occurs and seems to continue until each particle reaches a diameter of about 1 μm. Second, from this point, particles bond with each other to develop chain structures which grow, forming branches. Later, those structures compact in such a way that they develop a uniform pattern and none of the

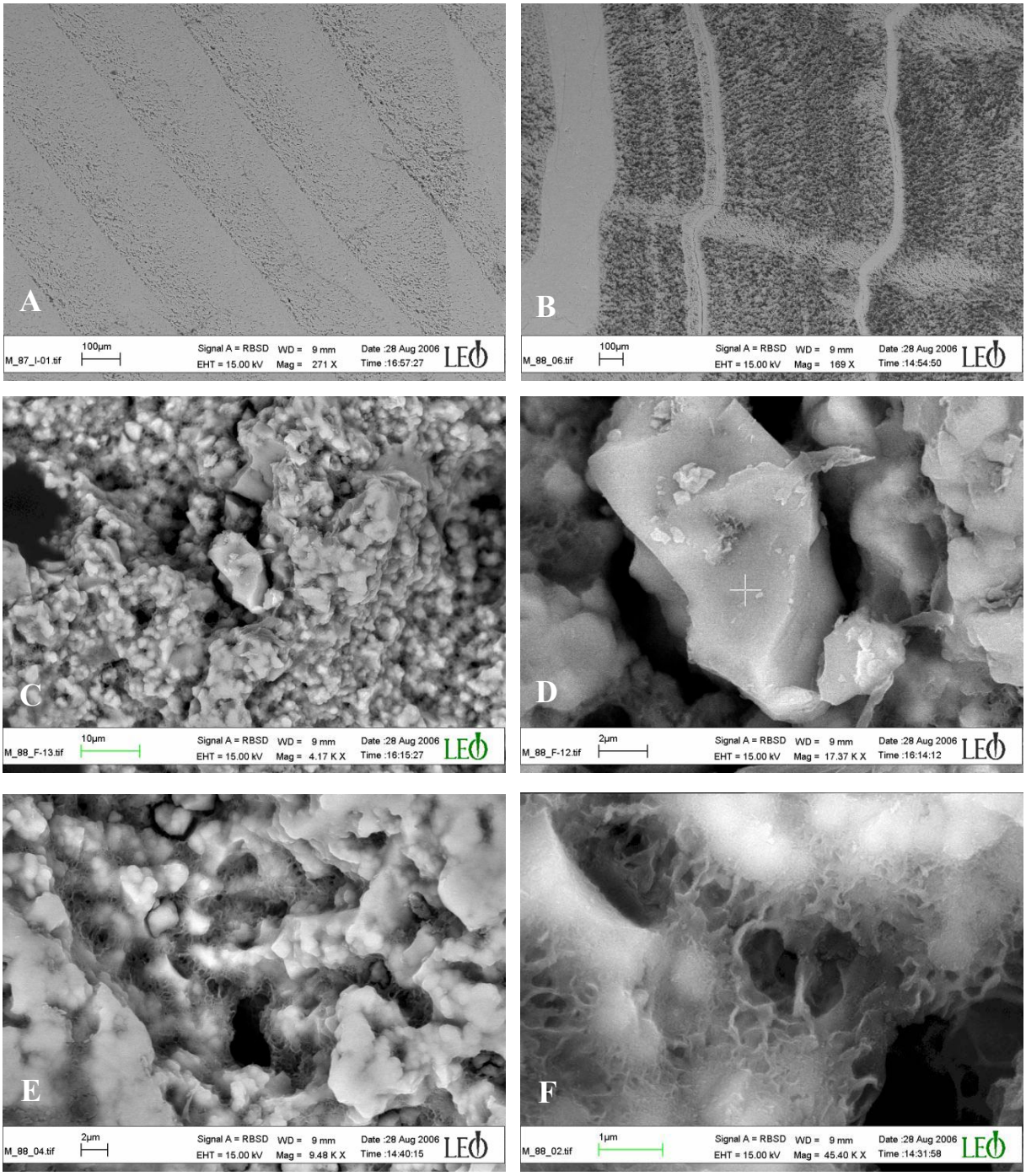

FIGURE 7: SEM micrographs

particles or chains can be observed. From here, the process seems to be interrupted and growth starts again. This process is illustrated in Figure 8.

The results of spot analyses performed by an X-ray energy dispersive spectrometer (EDS) are presented in Table 4. The sampling points were selected to be as representative as possible of the different types of textures described previously. The composition of each element is reported as its respective oxide. This is done conventionally, even when it is known that the oxides are probably not the most common form in which the element is present. The reason for this is that the stoichiometry calculations were performed on an oxide basis.

TABLE 4: Major element analysis of the scales; elements are listed as oxides; the compositions are recalculated to a 100% dry weight basis

Spot	18288 A1	18288 A2	18288 A4	Spec. 6	18288 C_edge	18288 C5	18288 C1-4	18288 xtal?	18288 E	18287 F1	18287 F m1	18287 F spec.	1828 F m2	18287 I1
Na_2O	-	1.13	-	-	-	0.45	-	0.84	0.98	-	0.42	-	-	-
MgO	2.24	6.18	2.88	-	3.79	2.22	2.13	3.26	13.76	2.49	5.63	2.04	1.46	1.57
Al_2O_3	4.04	3.48	3.56	5.69	4.16	4.24	4.00	3.86	4.47	3.50	4.20	3.79	4.12	3.80
SiO_2	56.52	54.13	51.98	55.95	56.22	55.20	51.74	57.60	56.30	53.96	58.88	52.00	51.03	52.79
K_2O	-	-	-	-	-	0.30	0.38	-	0.68	-	-	-	-	0.36
CaO	1.75	1.60	1.16	-	1.74	1.43	1.25	1.39	1.38	1.33	1.56	1.30	1.13	1.29
MnO	5.82	6.45	7.19	5.61	6.12	6.01	6.63	5.84	6.76	7.67	12.47	7.19	5.49	7.02
FeO	29.64	27.04	32.92	32.74	27.97	30.15	33.89	27.21	15.66	31.05	16.84	33.69	36.78	33.17
Total (%)	*100*	*100*	*100*	*100*	*100*	*100*	*100*	*100*	*100*	*100*	*100*	*100*	*100*	*100*

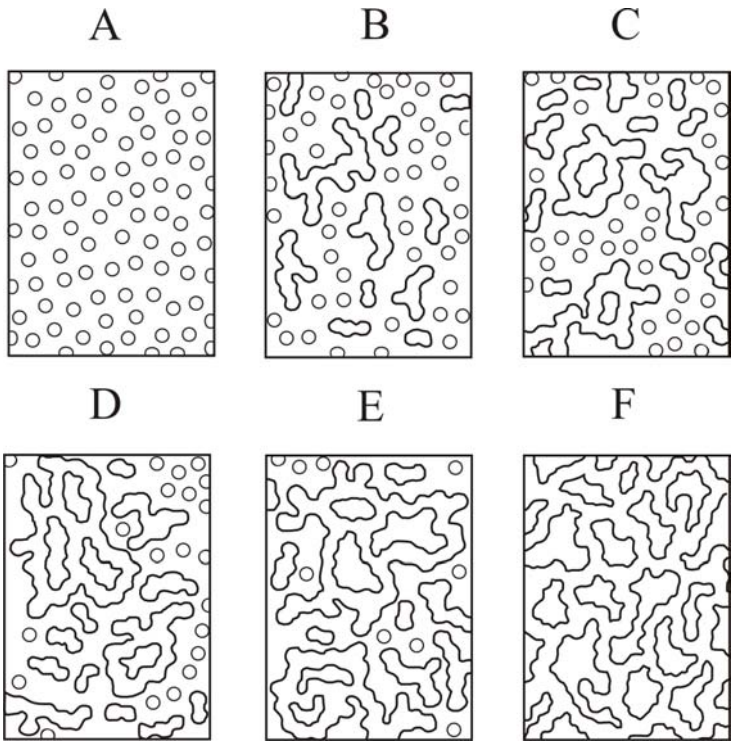

FIGURE 8: Diagram that shows the formation mechanism of the scales. From A to F, the particles grow until they reach a certain diameter and then bond to each other resulting in chains; later, those chains become a compact structure (Iler, 1979).

It is observed that scales consist mainly of silicon, oxygen, iron and manganese. Other elements like aluminium and magnesium are present but are not very important. Calcium, sodium and potassium appear only in small quantities. There were no significant differences in chemical composition between the porous and compact layers.

In conclusion, the laminations present on the scales seem to be due to changes in the texture rather than changes in the chemical composition. Differences in texture are probably due to variations in the growth rate of silicate which could be attributed to pH changes over time. It is well known that pH plays an important role in the kinetics of silicate deposition.

4.5 Stoichiometry of the scale compound

Based on weight percentages of the constituent oxides given by EDS spot analyses, the calculation of a chemical empirical formula was performed. The details of this procedure and its theoretical background can be consulted in Deer et al. (1992). The calculations were done with the following considerations:

- Because of the reducing conditions where scales were formed, most of the iron, if not all, must be in the form of ferrous ion (Fe^{+2}).
- Based on chemical and EDS spot analyses, the main compounds of scales are silicon, oxygen and iron.
- Because amorphous minerals do not have a crystalline structure, they can easily accept other anions and cations that would not occur in the crystallized phase. That, in fact, could explain the presence of other elements in minor quantities.
- The macroscopic description of scales formed at Miravalles agrees with those belonging to amorphous iron silicates reported in other places around the world.
- Those facts point out that the phase under these considerations could be an amorphous ferrous silicate.
- The calculations were based on 11 oxygen atoms or equivalents per formula unit.

The atomic ratios between the main cations in scales (iron, manganese and magnesium) and silicon are presented in Figure 9. The results of some authors which have reported the occurrence of iron silicate scales around the world are also presented for comparison. It can be observed that the stoichiometry of scales at Miravalles is intermediate between nontronite ($Na_{0.3}Fe^{+++}{}_2(SiAl)_4O_{10}(OH)_2 \cdot n(H_2O)$) and minnesotaite ($(Fe^{++},Mg)_3Si_4O_{10}(OH)_2$). Some iron oxides were plotted on the y-axis in order to represent different iron oxidation states. Since the scales plot in the area defined by the lines that connect amorphous silica with FeO and magnetite, it is very likely that the iron present in the scales is in the form of ferrous (Fe^{2+}) iron, as was supposed. All this led to the conclusion that the compound present in the scales at Miravalles is an amorphous ferrous silicate which has a stoichiometry similar to minnesotaite. Magnesium can substitute part of the iron in its formula. Actually, minnesotaite is very similar to the iron end member of talc ($Mg_3Si_4O_{10}(OH)_2$), which is sometimes referred to as ferrous talc (Deer et al., 1992).

4.6 Thermodynamic considerations

Having defined the stoichiometry of the scale phase, an expression for its dissolution can be expressed as:

$$6H^+ + Fe_3Si_4O_{10}(OH)_2 \Leftrightarrow 3Fe^{2+} + 4SiO_2 + 4H_2O \qquad (4)$$

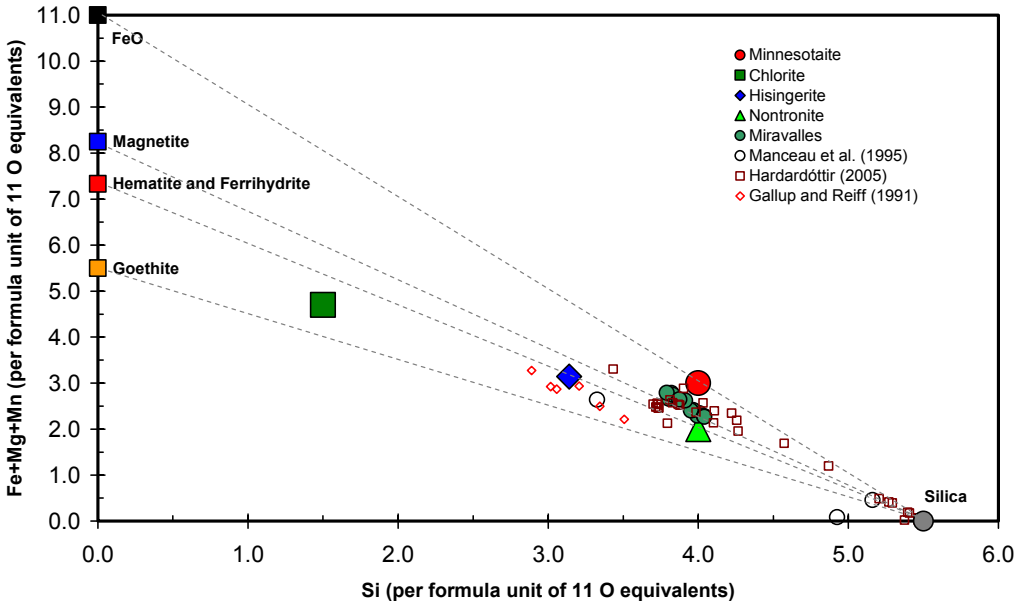

FIGURE 9: Atomic ratios between major cations and silicon in scales at Miravalles

The equilibrium constant of Reaction 4 can be written as:

$$K = \frac{(a_{Fe^{2+}})^3 \cdot (a_{SiO_2})^4 \cdot (a_{H_2O})^4}{(a_{H^+})^6 \cdot (a_{Fe_3Si_4O_{10}(OH)_2})} \quad (5)$$

Assuming that the activities of the aqueous and the solid phases are equal to 1, Equation 5 becomes:

$$K = \frac{(a_{Fe^{2+}})^3 \cdot (a_{SiO_2})^4}{(a_{H^+})^6} \quad (6)$$

It can be deduced from Equation 6 that the precipitation of scales is a reaction that strongly depends on the activity of H^+ or, in other words, the pH. Equation 6 will be used to evaluate the conditions under which the scales form.

5. GEOCHEMICAL MODELLING

In this chapter, the criteria for selecting the wells and their fluid samples for further consideration will be explained in conjunction with the methodology for the assessment of the deep fluid compositions. Then, the results of both actual and simulated mixing scenarios will be described.

5.1 Wells involved in the present study

The wells involved in this study are those that contribute to the formation of the scales in the surface pipelines where two-phase fluids are transported to separation station 2 (Figure 3). The scales formed during an approximate 3 month period, between July and October 2004. During this period, a mixture of fluids from PGM-66 and PGM-17 was combined with the PGM-19 acid fluids at U-20. At that point, scales started to deposit. The presence of the scales was also observed at U-21, where the fluids from PGM-03 combined with the mixture downstream from the previous addition of PGM-19 fluids. At separation station 2, scale deposition occurred inside separators and water tanks. During that time, well PGM-46 was integrated to separation station 2. At U-601, where PGM-46 fluids mixed with the ones coming from the addition of PGM-03 fluids, scales also deposited.

For the calculation of deep fluid compositions and mineral saturation states, liquid phase samples collected between 2003 and 2005 at atmospheric pressure, and gas samples collected at different pressures from wells PGM-03, PGM-17, PGM-66 and PGM-19, were selected in order to be as representative as possible of the normal operating conditions (Table 5). Fluids from wells PGM-03, PGM-17 and PGM-66 are very similar with respect to their chemical composition. Although iron was not analyzed in samples from wells PGM-03, PGM-17 and PGM-66, it is usually in low concentrations ($\leq$ 0.05 ppm) in neutral fluids. The neutralizing system at PGM-19 was not operating on September 18th, 2005, while samples were collected. On the other hand, samples from October 13th, 2005, were collected during normal operating conditions. It can be seen that there are big differences with respect to iron concentrations and pH between these samples.

For practical reasons, normal operating conditions will be defined as a state of production in which the well is integrated to the steam gathering system and produces at maximum flowrate (except in a few cases) in order to deliver the maximum steam flow and thus power output to the power station. Cases where samples were collected close to a mechanical maintenance operation in the well or when the inhibition system was not operating were not considered. A normal operating condition is that in

TABLE 5: Typical chemical compositions of fluids of the wells involved in the formation of the scales at atmospheric pressure or 98°C

Well	**PGM-03**	**PGM-17**	**PGM-19**		**PGM-66**
Date	03.02.06	04.02.06	18.09.05	13.10.05	04.02.06
Sep. pressure (bar-a)	0.94	0.94	0.94	0.94	0.94
Well head press. (bar m.)	10.64	8.70	8.30	7.70	10.34
pH	7.73	8.17	3.05	5.76	7.99
Cond. (µS/cm)	14105	14290	13330	12630	13265
Na (ppm)	2755	2828	2371	2505	2552
K (ppm)	311	322	304	300	283
Ca (ppm)	90	89	42	37	76
Mg (ppm)	-	0.05	7.15	7.13	0.05
Total Fe (ppm)	-	-	24.10	0.49	-
Cl (ppm)	4493	4544	3935	3973	4171
SO_4 (ppm)	57	53	322	326	57
HCO_3 (ppm)	19	15	-	1.50	45
B (ppm)	70	70	68	67	65
H_2S (ppm)	-	-	-	-	-
Total SiO_2 (ppm)	545	567	-	576	562
Mono. SiO_2 (ppm)	528	-	576	544	527
TDS (ppm)	8550	8575	7935	7470	8110
CO_2 (mmoles/kg)	241.28	72.25	74.83	117.77	145.07
H_2S (mmoles/kg)	1.57	0.78	1.47	1.79	0.84
N_2 (mmoles/kg)	3.36	1.16	1.12	0.67	1.34
CH_4 (mmoles/kg)	0.17	0.07	0.05	0.08	0.10
H_2 (mmoles/kg)	0.46	0.04	0.08	0.10	0.05
Total	246.83	74.30	77.55	120.41	147.41
% in steam	1.08	0.32	0.34	0.53	0.65
$T_{Na/K}$ (°C)	228	228	239	233	226
$T_{Na/K/Ca}$ (°C)	229	230	243	240	227
$T_{quartz\ mpv}$ (°C)	230	231	236	232	229
$T_{meas.}$ (°C)	-	239	230(?)	230(?)	236
Enthalpy (kJ/kg)	1246	1032	1140	1140	1067

which wells are operated most of the time. The reason for those criteria is that for many years at Miravalles, huge differences in concentrations of many components, both in liquid and gaseous phases between samples collected at different operation conditions, have been observed. Samples from PGM-46 were not taken into account because this well is normally integrated to separation station 6, but only in a few cases to separation station 2.

Because only PGM-19 is acidic, the point of interest is the intersection where the two types of fluids mix. Fluid temperatures in the pipeline are estimated to be between 190 and 200°C (Sánchez, pers. com.). For calculating purposes, an average temperature of 195°C was used.

5.2 Assessment of the deep fluid composition

In order to calculate the deep fluid composition, liquid phase samples collected at atmospheric pressure (98°C) and gas samples recalculated to those conditions were input to WATCH chemical speciation program version 2.3 (2004). The program reads chemical analyses of water, gas, and steam condensate samples, collected at the surface, and computes the chemical composition of downhole, or aquifer fluids at a selected reference temperature. This includes the pH, aqueous speciation, partial pressures of gases, redox potentials, and activity products for mineral dissolution reactions. The

background of the program and the general methods of calculation used are described by Arnórsson et al. (1982).

PGM-03 and PGM-19 present excess enthalpy, which means the measured discharge enthalpy is higher than the value that could be expected based on the measured temperature in the well below the level of first boiling (aquifer temperature). The excess enthalpy refers to a situation when the steam to water ratio in a well discharge is higher than can be produced by pressure drop of the initial aquifer fluid. According to Arnórsson (2000) this can be due to 1) flow of heat from the rock to the boiling water that flows through the zone of depressurization to the well and 2) phase segregation, in which steam flows into the well but the water is partially or totally retained in the aquifer. In Miravalles, the cause of excess enthalpy is deep boiling in the formation, resulting in phase segregation.

For calculating purposes, the downhole temperature measured in dynamic temperature logs was utilized as the reference temperature value for wells PGM-17 and PGM-66. For PGM-03, the reference value was the temperature of the quartz geothermometer of Fournier (1977) and in the case of PGM-19, an estimated temperature based on dynamic temperature logs ran before excess enthalpy was detected in the well.

The scheme followed with the input data from each well in the WATCH program was:

1) Calculation of the aquifer composition at the reference temperature.
2) Performance of boiling steps from the reference temperature to the following sequence of temperatures: 195, 170, 165, 159 and 98°C. The boiling process was assumed to be adiabatic and degassing in equilibrium (degassing coefficient = 1).
3) After the last boiling step was performed (98°C), the calculated composition of the fluid was compared with the analysis of the sampled fluids at the same temperature, in order to evaluate how appropriate the reference temperature value was.
4) Saturation indices of amorphous silica and pH values were calculated because initially it was inferred that those parameters were playing an important role in the scaling problem studied in this work.
5) Special attention was paid regarding fluid composition calculated at 195°C, because that is the estimated temperature of the mixing point between neutral and acidic fluids. Also, the composition at that temperature would be used in the mixing calculations, explained later in this study.

5.3 Saturation indices

The chemical composition of the samples obtained after simulating boiling to 98°C using WATCH were very close to the analyses of the samples collected at the same temperature. Saturation indices calculated by WATCH showed that amorphous silica did not reach super saturation above 98°C in any of the wells considered in this study (Figure 10). Similarly, there were no significant differences in the degree of saturation of calcite, amorphous silica and also pH within the time interval considered (2003 – 2005). If two or more solutions at the same temperature were under saturated with respect to amorphous silica, then the resulting mixture would also be under saturated. As a result, the scales formed at Miravalles could not be related to amorphous silica.

5.4 Mixing calculations

Before describing the work carried out for modelling fluid mixing, some considerations must be explained. It is clear at this point that scales formed because the mixing of fluids with different chemical compositions led to a pH increase. That, added to the fact that acidic fluids are richer in iron than neutral fluids, sets the scenario for the amorphous iron silicate to precipitate. However, it has to

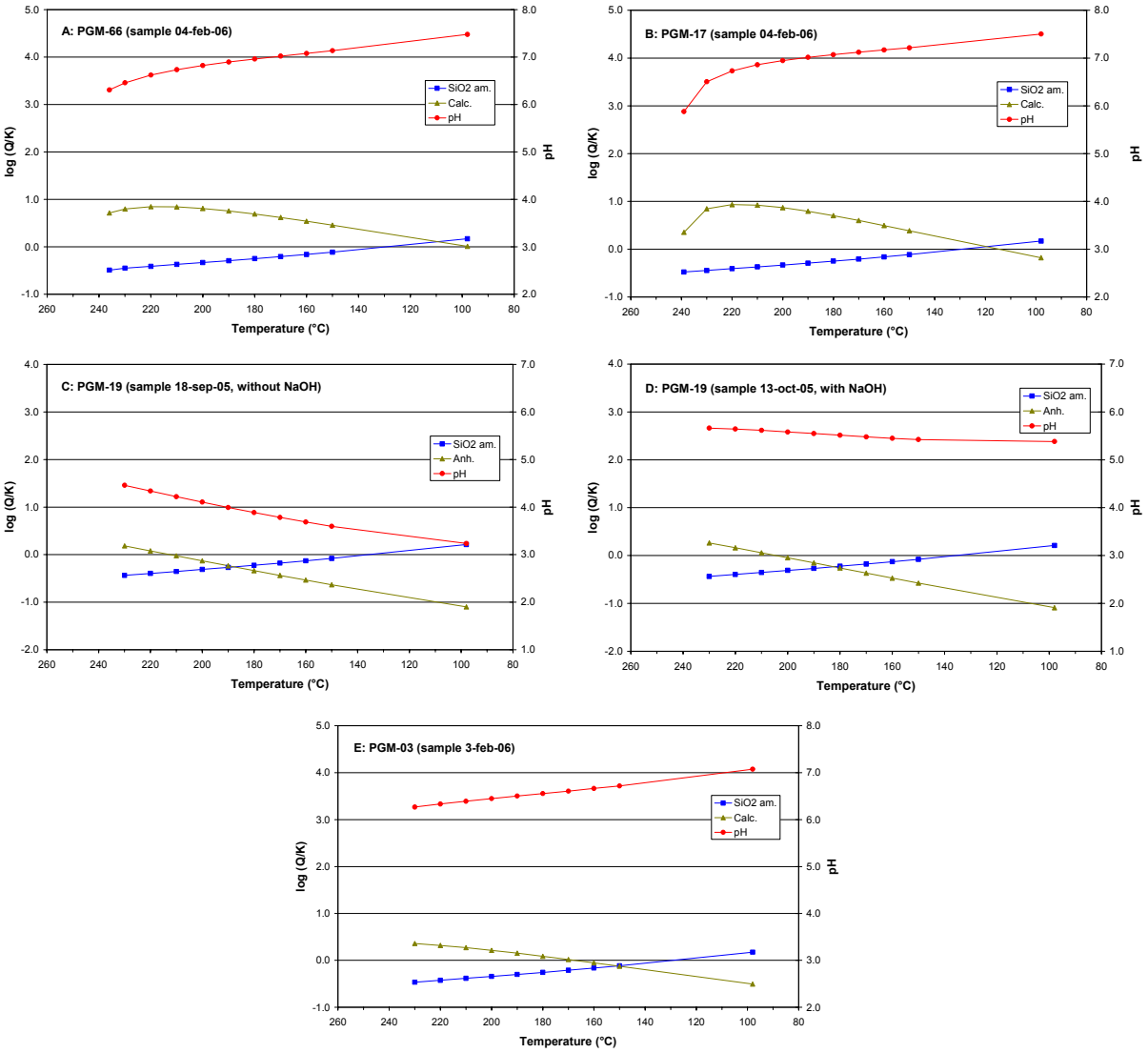

Figure 10: Saturation indices of calcite, anhydrite and pH of the fluids from wells PGM-66, PGM-17, PGM-19 and PGM-03; notice that in PGM-19 different producing conditions are compared (with and without NaOH)

be taken into account that the main problem there is the pH increase. That can be deduced from the expression of the equilibrium constant (Equation 6) and observing that it is very sensitive to changes in pH.

Since the scaling begins at the point where neutral fluids from wells PGM-66 and PGM-17 mix with acidic fluids coming from PGM-19, only this case was analyzed. Furthermore, to simplify things, only the fluids from PGM-17 were taken into account for modelling. This is justified because the fluids of wells PGM-17 and PGM-66 are chemically very similar (Table 5) and also because no scales have formed in the pipelines where the mixture of fluids from wells PGM-66 and PGM-17 occurs.

Chemical composition data of fluids boiled to 195°C from PGM-17 and PGM-19, taken from WATCH, were run in EQ3NR (v. 7.0) aqueous speciation software. EQ3NR, like WATCH, computes the distribution of chemical species in the solution, including simple ions, ion pairs, and complexes, using standard state thermodynamic data and various equations which describe the thermodynamic activity coefficients of these species. More details of this software can be reviewed in Wolery (1992). The reason for using EQ3NR was that its results serve as an input file to EQ6 (v. 7.0), a reaction path

modelling code for aqueous geochemical systems. Complete information of this software is given by Wolery and Daveler (1992).

Reaction path modelling represents the process by which a set of irreversible reactions proceed to a state of thermodynamic equilibrium (Wolery and Daveler, 1992). Irreversible reactions might begin in a metastable equilibrium state and end in a stable equilibrium state, but in between these states the system must necessarily pass through states of disequilibrium. The general aim is to be able to trace what happens during irreversible reactions or processes, such as dissolution or precipitation of minerals, mixing solutions, cooling or heating systems (Zhu and Anderson, 2002).

There are many reaction path models. Mixing or titration modelling simulates the process of the addition of a reactant into a system. The reactant can be a mineral, a chemical reagent, a glass, a gas, another aqueous solution, a rock, or anything for which the chemical stoichiometry can be defined (Zhu and Anderson, 2002). This kind of model is the most suitable for understanding the processes that occur during the mixing between fluids from wells PGM-17 and PGM-19.

In order to have a more representative view of the situation, mixing experiments between PGM-17 and PGM-19 were carried out with samples belonging to the same time period. For example, it would give a dubious scenario to mix fluids sampled at PGM-17 during 2003 with fluids sampled at PGM-19 during 2006. During each run in EQ6, fluids from PGM-17 and PGM-19 were mixed at 195°C. Fluids from PGM-17 were titrated with fluids from PGM-19 until a mixture of equal parts of each was achieved. On the other hand, in order to have the whole spectrum of the mixing experiment, fluids from PGM-19 were titrated with fluids from PGM-17. Thus, two runs per mixing experiment were done.

An important consideration concerning the paths followed by the code of EQ6 software, in order to reach a state of equilibrium, is related to the precipitation of secondary phases. The default condition is that EQ6 will precipitate any phase to avoid supersaturating the aqueous solutions, no matter if one phase, geochemically speaking, makes more sense that another. However, in the modelled mixing experiments conducted in this study, the precipitation of all minerals was suppressed.

The activities of Fe^{2+}, SiO_2 and H^+ resulting from each run were used to calculate the reaction coefficient (Q) of the dissolution reaction of the scale phase at every step of the reaction path, as showed in Equation 7.

$$Q = \frac{(a_{Fe^{2+}})^3 \cdot (a_{SiO_2})^4}{(a_{H^+})^6} \tag{7}$$

If a given reaction is in equilibrium, then $Q = K$. A convenient way to evaluate the state of saturation of an aqueous solution, with respect to a mineral or phase, would be to calculate the saturation index (Q/K). The search for K for minnesotaite in literature was unsuccessful. However, it does not imply that important deductions about saturation states of amorphous minnesotaite-like compounds cannot be derived in combination with observations carried out in pipelines and mixing proportions.

5.4.1 Actual mixing scenarios

The results of mixing experiments carried out by EQ6 are presented in Figure 11. The log Q of the scale phase is plotted against the mixing ratio between PGM-17 and PGM-19. All of the PGM-19 samples, except from September 2005, correspond to periods when those fluids were neutralized by means of NaOH. At the extremes of the x-axis, the end members of the mixture between PGM-17 and PGM-19 are plotted. Iron content in PGM-17 fluids is in non-detectable concentrations, thus log Q of the scale phase at PGM-17 extreme is not defined. In the starting solutions, the scale phase was assumed to be under saturated. Otherwise, scales would have been observed in two-phase pipelines on

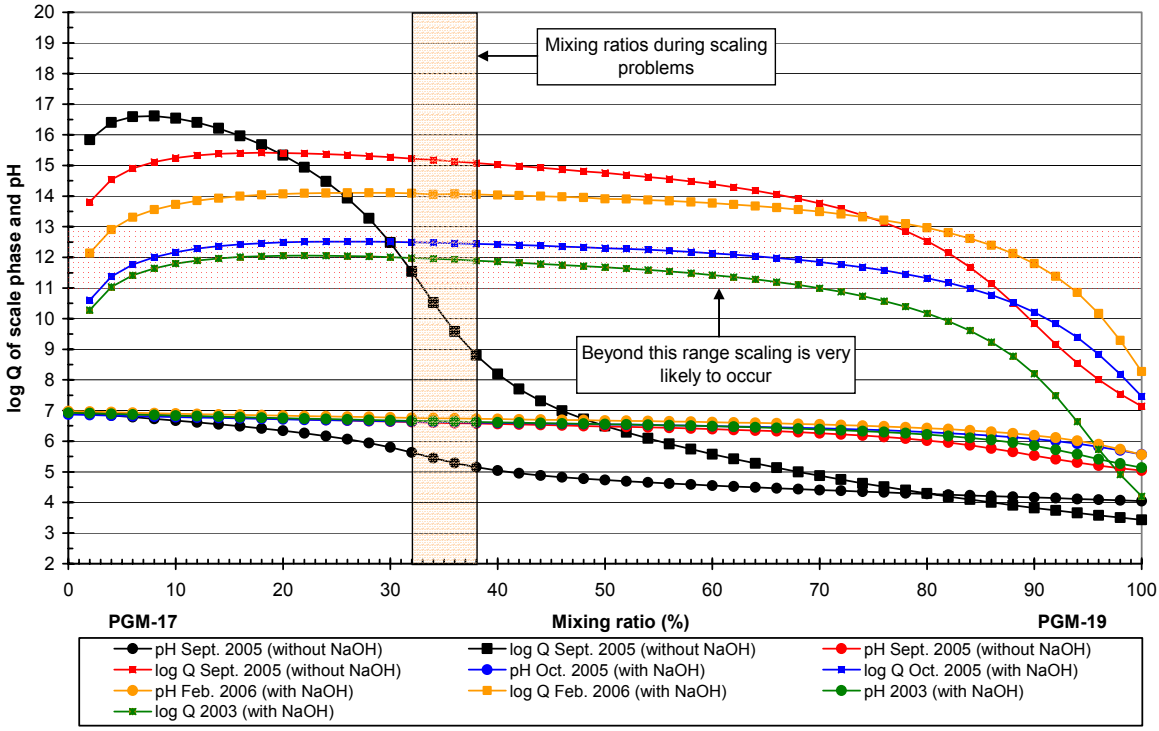

FIGURE 11: Mixing models between PGM-17 and PGM-19 fluids;
the shaded area represents scale phase over saturation threshold

the way to the mixing point between those wells. On the other hand, PGM-19 solutions were richer in iron. Concentrations between 0.23 and 0.81 ppm were present in neutralized samples and between 3.66 and 19.49 ppm in non-neutralized samples.

In the case of neutralized PGM-19 samples, log *Q* rapidly increased in the first mixing stages of PGM-19 with PGM-17, until a mix ratio of 80% and 20%, respectively, existed. Beyond that point both log *Q* and pH slowly increased. In Figure 11 the mixing ratios that represent the conditions prevailing when the scales formed at the mixing point between PGM-19, PGM-17 and PGM-66 fluids are illustrated. According to Sánchez (pers. com.) at that site there were 100 kg/s delivered by PGM-66, 100 kg/s by PGM-17 and the contribution of PGM-19 was about 110 kg/s. That makes 64.6% of neutral fluids and 35.4% of acidic fluids. Because scaling occurred, it is deduced that over saturation of the minnesotaite-like phase existed at these mixing conditions.

Considering that in this experiment the starting solutions were under saturated with respect to the scale phase, and that at a certain point of their mixing path the mixture became over saturated, it is inferred that the value of log *K* would range between 11 and 13 on the y-axis, thus $11 \leq \log K \leq 13$ at 195°C. Therefore, if log *Q* values exceeded this range, scaling was very likely to occur.

Results from the mixing experiments show that the scale phase over saturation was reached with the slightest addition of PGM-19 fluids to PGM-17 fluids, until the mixing ratio contained more than 70% of PGM-19 fluids. Those ratios varied, of course, and depended on the degree of neutralization of PGM-19 fluids. An interesting situation appeared in the mixing experiment that corresponded to the samples taken on September 2005. For a short period, PGM-19 was not being neutralized, so the pH of the mixing fluids was lower compared to the other mixing experiments. Furthermore, the scale phase under saturation remained until PGM-19 fluids constituted more than 32% of the mixture. That behaviour suggests that a pH decrease would result in a decrease of the saturation of the scale phase.

Iron, silica and pH play an important role in the formation of the scales. pH is, in fact, the most sensitive parameter and the only one that can be directly controlled by means of neutralization. At this

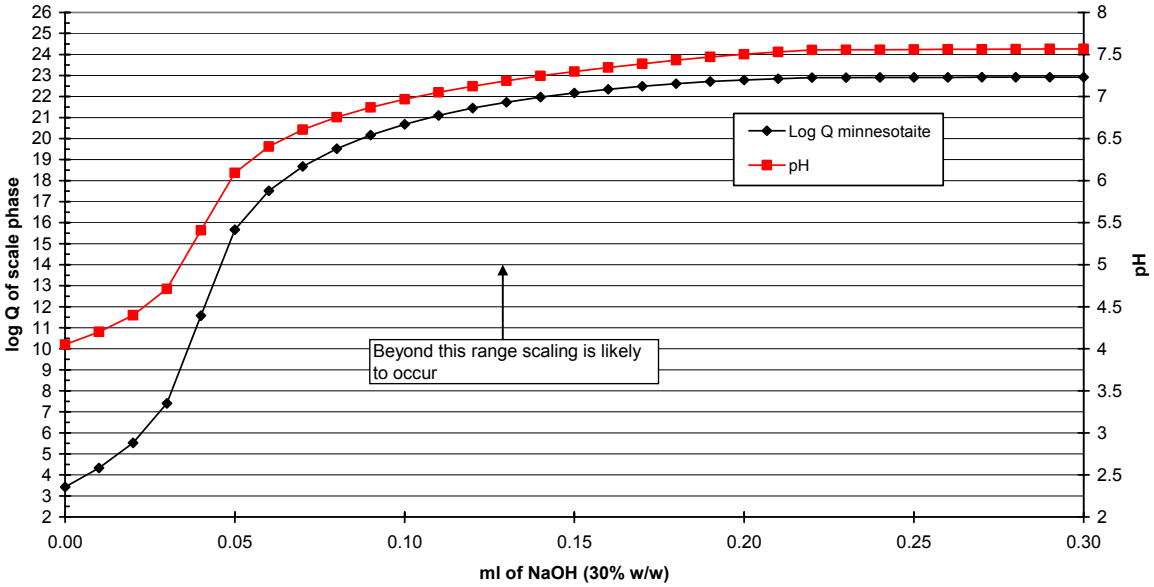

FIGURE 12: Titration of a non-neutralized fluid with NaOH (30% w/w) at 195°C

point, the question arises about how the degree of saturation of the scale phase could change if an acid solution of PGM-19 was neutralized.

The result of a titration experiment carried out by EQ6 is present in Figure 12. The NaOH solution utilized was at a concentration of 30% w/w, similar to the one employed for deep neutralization treatments at Miravalles. The PGM-19 titrated solution corresponded to a non-neutralized sample taken on September 2005, with an initial iron content of 19.49 ppm. The titration was run at a temperature of 195°C. According to scaling and corrosion rate studies performed on acid fluids at different pH values of neutralization (Rodríguez and Sánchez, 2004; NEDO, 2004), it is very likely that beyond a pH of 5.0, scaling will occur at the same temperature conditions as of the titration experiment made here. Taking into account all those observations, the log *Q* of the scale phase seems to be in a range from 14 to 15.

These results are somewhat higher than what was found in the mixing experiments. However, it has to be considered that this case is different with respect to the mixing experiment because the iron contents here were much higher. Therefore, it is expected that the log Q values would attain higher values sooner than in the mixing experiments. The most important conclusion of this experiment is that this process resembles the case where neutralization is carried out inside an acidic well in order to avoid corrosion.

5.4.2 Simulated mixing scenarios

With the goal in mind of finding a solution that could solve scaling problems due to mixing between neutral an acidic fluids, some scenarios were modelled. One possible solution involved acidifying fluids from neutral wells. That would involve performing this operation in wells PGM-17, PGM-66 and PGM-03. In order to simplify things, the mixing models were done as if only PGM-17 fluids were acidified.

Three scenarios considered mixing acidified PGM-17 fluids to the next pH values: 6.5, 6.0 and 5.5, with neutralized fluids from PGM-19. The results are presented in Figure 13. The pH 5.5 and 6.0 scenarios show curves that run well below the over saturation threshold of the scale phase. On the other hand, under the pH 6.5 scenario, the curve touches that threshold; therefore, scaling might occur under those conditions. One must realize that all these mixing models only give a starting point for future field tests. The results of these experiments are theoretical and must be confirmed by scaling and corrosion rate tests using coupons in specific location in the pipelines.

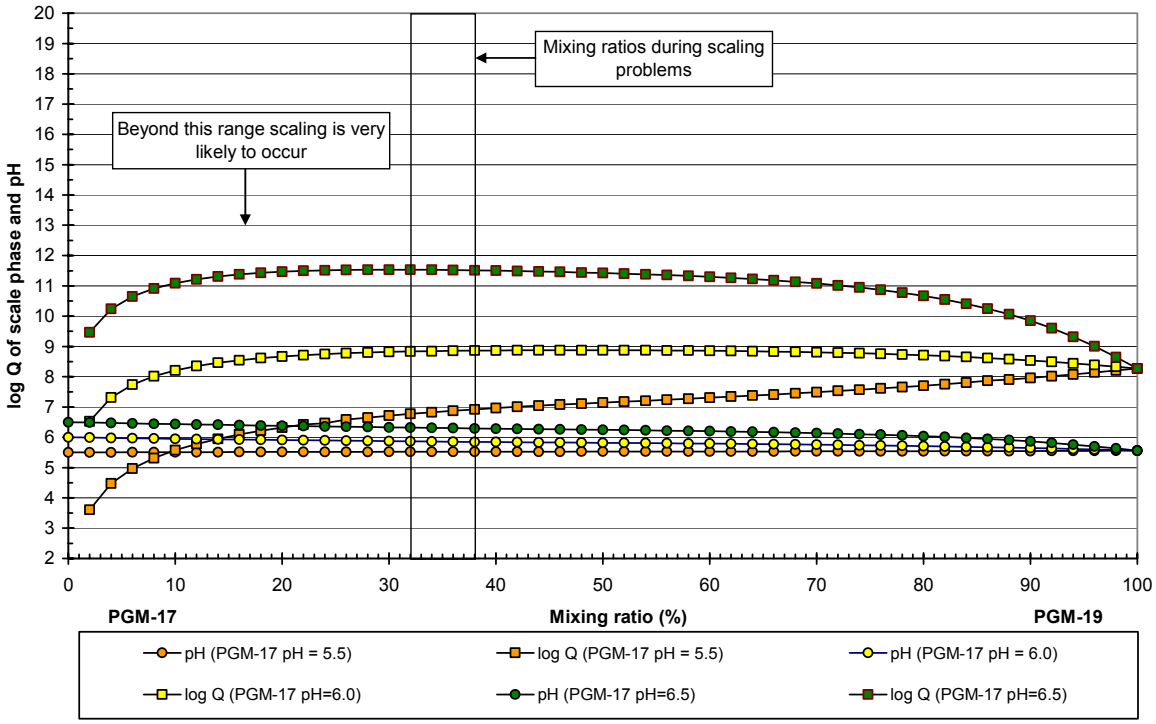

FIGURE 13: Mixing models with pH value scenarios of 5.5, 6.0 and 6.5

6. CONCLUSIONS

6.1 Conclusions

Chemical and EDS analyses determined that scales formed at Miravalles as a result of mixing neutral fluids with acidic ones, are mainly composed of silicon, oxygen and iron. That composition corresponds to a ferrous silicate with a stoichiometry very similar to minnesotaite ($(Fe^{++},Mg)_3Si_4O_{10}(OH)_2$).

XRD patterns suggested that the scales are mainly amorphous or poorly crystallized. Because of the amorphous nature of scales, they can easily accept many other ions into the bulk mass, which could explain the presence of other elements in minor quantities.

SEM micrographs showed that the layered structures observed in hand specimens of scales are due to textural differences, rather than chemical differences. The dark layers present a compact texture while the light brown layers develop a porous texture consisting of particle aggregates.

The consistent chemical composition of the scales made it possible to define a reaction for the dissolution of the scale phase. Iron, silica and pH control the precipitation of scales, but the last is the most sensitive parameter and the one that can be directly controlled. A high iron content provided by PGM-19 acidic fluids and a pH increase that occurs during the mixing between those fluids with neutral ones, are the key factors that control the saturation state of the scale phase.

A titration experiment, in which a PGM-19 fluid was neutralized with NaOH, is the same case as when pH is raised too much inside an acid well in order to avoid corrosion.

The mixing experiments between neutral and acidic fluids determined a threshold of log *K* of the scale phase between 11 and 13. Above this range, the probabilities of over saturation of this compound are very high. Decreasing pH values of neutral fluids seems to be a feasible solution in order to avoid scaling. According to the mixing models performed with a pH of 6.0, no scaling seems to occur. A minimum value could be around 5.0, according to the corrosion test performed at PGM-07 in 2002.

6.2 Recommendations

- Decreasing the pH of neutral fluids with an acid (e.g. HCl) to a maximum value of 6.0 is recommended.

- Corrosion and scaling rate studies are, however, necessary in order to optimize this value and reach a good balance between corrosion and scaling.

- Additional studies of the scale such as IR and Mössbauer spectroscopy would be valuable to further investigate the nature of the scales.

ACKNOWLEDGEMENTS

First of all, I would like to express my sincere gratitude to the director of the UNU-GTP, Dr. Ingvar B. Fridleifsson and also to Mr. Lúdvík S. Georgsson, deputy director. Their goal of training young professionals has, and still does, contribute to the development of many countries. My deepest thanks to Mrs. Gudrún Bjarnadóttir and to Ms. Thórhildur Ísberg, for their efficient and invaluable help during my training in Iceland. I am very grateful to my supervisor Dr. Thráinn Fridriksson for our rich discussions. His excellence guidance and endless patience were of great value during this investigation. I would like to give thanks to Ms. Anette K. Mortensen. Her professional work with SEM was one of the keystones of this study, and her suggestions for improving this report were important; to Sigurdur Jónsson, Steinthór Níelsson and Snorri Gudbrandsson for their assistance with the XRD; and to Bjarni R. Kristjánsson and Gunnlaugur M. Einarsson for their assistance with the photos in the stereoscope. Finally, thanks to my colleagues at ICE, especially to Mr. Eddy Sánchez who was one of the people who made training in Iceland possible. His comments during this investigation were also helpful.

REFERENCES

Andritsos, N., and Karabelas, A.J., 1991: Sulphide scale formation and control: the case of lead sulphide. *Geothermics, 20*, 343-353.

Arnórsson, S., 2000: Assessment of reservoir fluid composition form wet steam well data. In: Arnórsson, S (ed.), *Isotopic and chemical techniques in geothermal exploration, development and use.* International Atomic Energy Agency, Vienna, 212-227.

Arnórsson, S., Sigurdsson, S., and Svavarsson, H., 1982: The chemistry of geothermal waters in Iceland I. Calculation of aqueous speciation from 0°C to 370°C. *Geochim. Cosmochim. Acta, 46*, 1513-1532.

Castro, S. and Sánchez, E., 1998: *Production test of well PGM-07, Miravalles*. ICE, internal report (in Spanish), 11 pp.

Deer, W.A., Howie, R.A. and Zussman, J., 1992: *An introduction to the rock-forming minerals* (2nd ed.). Longman Scientific and Technical, Hong Kong, 696 pp.

Fortin, D., Grant Ferris, F. and Scott, S., 1998: Formation of Fe-silicates on bacterial surfaces in samples collected near hydrothermal vents on the Southern Explorer Ridge in the northeast Pacific Ocean. *American Mineralogist, 83*, 1399-1408.

Fournier, R., 1977: Chemical geothermometers and mixing model for geothermal systems. *Geothermics, 5,* 41-50.

Gallup, D.L., 1989: Iron silicate scale formation and inhibition at the Salton Sea geothermal field. *Geothermics, 18*, 97-103.

Gallup, D.L., 1993: The use of reducing agents for control of ferric silicate scale deposition. *Geothermics, 22*, 39-48.

Gallup, D.L. and Reiff, W.M., 1991: Characterization of geothermal scale deposits by Fe-57 Mössbauer spectroscopy and complementary X-ray diffraction and infra-red studies. *Geothermics, 20*, 207-224.

Hardardóttir, V., 2004: Major and trace elements in scales in pipes from well 9, Reykjanes, Iceland. *Proceedings of the 11th International Symposium on Water-Rock Interaction 2004, New York, USA,* Taylor & Francis Group, London, 1521-1525.

Hardardóttir, V., 2005: Sulfide scales from geothermal brine in wells at Reykjanes, Iceland. *Geological Society of America (GSA), Salt Lake City Annual Meeting, abstracts with programs, 37-7,* 452.

Hardardóttir, V., Ármannsson, H., and Thórhallsson, S., 2005: Characterization of sulphide-rich scales in brine at Reykjanes. *Proceedings of the World Geothermal Congress 2005, Antalaya, Turkey*, CD, 8 pp.

Hoyer, D., Kitz, K., and Gallup, D.L., 1991: Salton Sea unit 2: Innovations and successes. *Geotherm. Resources Counc., Transactions, 15*, 355-361.

ICE, 2004: Data relevant for the electrical sector (in Spanish). ICE, web page: http://www.grupoice.com/esp/ele/planinf/docum/datosgenerales_ele04.pdf (consulted on 18/09/2006).

Iler, R.K., 1979: The *chemistry of silica: solubility, polymerization, colloid and surface properties, and biochemistry.* John Wiley & Sons, New York, 866 pp.

Karabelas, A.J., Andritsos, N., Mouza, A., Mitrakas, M., Vrouzi, F., and Christanis K., 1989: Characteristics of scales from the Milos geothermal plant. *Geothermics, 18*, 169-174.

Kristmannsdóttir, H., 1984: Chemical evidence from Icelandic geothermal systems as compared to submarine geothermal systems. In: Rona, P.A., Boström, K., Laubier, L. and Smith, J.L.Jr. (eds.), *Hydrothermal processes at seafloor spreading centres*. Plenum Press, New York, 291-320.

Mainieri, A., 2005: Costa Rica country update report. *Proceedings of the World Geothermal Congress 2005, Antalaya, Turkey*, CD, 5 pp.

Manceau, A., Ildefonse, Ph., Hazemann, J.L., Frank, A.M., and Gallup D., 1995: Crystal chemistry of hydrous iron silicate scale deposits at the Salton Sea Geothermal Field. *Clays and Clay Minerals, 43*, 304-317.

Mercado S., Bermejo, F., Hurtado R., Terrazas B., and Hernández, L., 1989: Scale incidence on production pipes of Cerro Prieto geothermal wells. *Geothermics, 18*, 225-232.

Moya, P. and Sánchez, E., 2002: Neutralization system for production wells at the Miravalles geothermal field. *Geothermal Resources Council, Transactions, 26*, 667-672.

NEDO, 2004: *Experimental results of pH modifications for acid geothermal fluids in Miravalles, Costa Rica*. NEDO, report submitted to ICE, 20 pp.

Rodríguez, A., Sánchez, E., 2004: *Silica scaling and corrosion studies at well PGM-07, Miravalles*. ICE, internal report (in Spanish), 23 pp.

Sánchez, E., 1997: *Results of the neutralization of the well carried out in 1996 and proposal for their commercial use*. Miravalles Geothermal Power Project 16th Advisory Panel Meeting, ICE, internal report (in Spanish), 5 pp.

Sánchez, E., Guido, H., and Vallejos, O., 2000: Commercial production of acid wells at the Miravalles geothermal field, Costa Rica. *Proceedings of the World Geothermal Congress 2000, Kyushu-Tohoku, Japan,* 1629-1634.

Sánchez, E., Vallejos, O., Rodríguez, A., and Guido, H., 2005: Chemical treatments of fluids on the Miravalles geothermal field: investigation, application and its relationship with reservoir management. *Proceedings of the World Geothermal Congress 2005, Antalaya, Turkey*, CD, 7 pp.

Todaka, N., Akasaka, C., Xu, T., and Pruess, K., 2003: Modelling of geochemical interactions between acidic and neutral fluids in the Onikobe geothermal reservoir. *Proceedings of the 28th Workshop on Geothermal Reservoir Engineering, Stanford University, California*, 2003.

Vallejos, O., 1996: A conceptual reservoir model and numerical simulation for the Miravalles geothermal field, Costa Rica. Report 18 in: *Geothermal Training in Iceland 1996.* UNU-GTP, Iceland, 418-456.

Vega, E., Chavarría, L., Barrantes, M., Molina, F., Hakanson, E.C., and Mora, O., 2005: Geologic model of the Miravalles geothermal field, Costa Rica. *Proceedings of the World Geothermal Congress 2005, Antalaya, Turkey,* CD, 5 pp.

Wolery, T.J., 1992: *EQ3NR, a computer program for geochemical aqueous speciation-solubility calculations: theoretical manual, user's guide and related documentation (version 7.0)*. Lawrence Livermore National Laboratory, California, USA, 246 pp.

Wolery, T.J., and Daveler, S.A., 1992: *EQ6, a computer program for reaction path modelling of aqueous geochemical systems: theoretical manual, user´s guide, and related documentation (version 7.0).* Lawrence Livermore National Laboratory, California, USA, 338 pp.

Zhu, C., and Anderson, G., 2002: *Environmental applications of geochemical modelling*. Cambridge University Press, U.K., 284 pp.